

# Generating and manipulating quantized vortices on-demand in a Bose-Einstein condensate: A numerical study

B. Gertjerenken,<sup>1,2</sup> P. G. Kevrekidis,<sup>1,3</sup> R. Carretero-González,<sup>4,\*</sup> and B. P. Anderson<sup>5</sup>

<sup>1</sup>*Department of Mathematics and Statistics, University of Massachusetts Amherst, Amherst, Massachusetts 01003-9305, USA*

<sup>2</sup>*Institut für Physik, Carl von Ossietzky Universität, D-26111 Oldenburg, Germany*

<sup>3</sup>*Center for Nonlinear Studies and Theoretical Division, Los Alamos National Laboratory, Los Alamos, New Mexico 87544, USA*

<sup>4</sup>*Nonlinear Dynamical Systems Group, Computational Science Research Center, and Department of Mathematics and Statistics, San Diego State University, San Diego, California 92182-7720, USA*

<sup>5</sup>*College of Optical Sciences, University of Arizona, Tucson, Arizona 85721, USA*

(Received 20 August 2015; published 1 February 2016)

We numerically investigate an experimentally viable method for generating and manipulating on-demand several vortices in a highly oblate atomic Bose-Einstein condensate (BEC) in order to initialize complex vortex distributions for studies of vortex dynamics. The method utilizes moving laser beams to generate, capture, and transport vortices inside and outside the BEC. We examine in detail this methodology and show a wide parameter range of applicability for the prototypical two-vortex case, as well as case examples of producing and manipulating several vortices for which there is no net circulation, corresponding to equal numbers of positive and negative circulation vortices, and cases for which there is one net quantum of circulation. We find that the presence of dissipation can help stabilize the pinning of the vortices on their respective laser beam pinning sites. Finally, we illustrate how to utilize laser beams as repositories that hold large numbers of vortices and how to deposit individual vortices in a sequential fashion in the repositories in order to construct superfluid flows about the repository beams with several quanta of circulation.

DOI: [10.1103/PhysRevA.93.023604](https://doi.org/10.1103/PhysRevA.93.023604)

## I. INTRODUCTION

The realm of atomic Bose-Einstein condensates (BECs) [1–3] has presented a pristine setting where numerous features of the nonlinear dynamics of quantized vortices, vortex lattices, and other vortex distributions can be both theoretically studied and experimentally observed. Research in this domain has enabled observations of, for example, precession and excitation of few vortices [4–10], collective excitations and dynamics of vortex lattices [11–15], decay of multiply quantized vortices into singly quantized vortices [16,17], decay of dark solitons into vortices and vortex rings [18–20], and generation of quantum turbulence [21,22]. Additionally, experimental efforts directed towards new methods of vortex detection [8,23] are motivated by the need for direct measurements of the dynamics of arbitrary distributions of vortices. These, and numerous other experiments [24], demonstrate enormous progress towards developing a more complete understanding of vortex dynamics in BECs.

Nevertheless, to the best of our knowledge, there has not been an experimental demonstration of a method to construct at will arbitrary (topological charge, as well as spatial position) distributions of more than two vortices in a BEC. Such a method would enable detailed experimental studies of interactions of vortices with each other, with sound, and with trap impurities. New methods to study the evolution of many-vortex states involving quantum turbulence, as well as chaotic vortex dynamics [25–27], would be available, and the role of dissipation in superfluid dynamics could be more precisely determined based on experimental data. Here we extend a proof-of-principle experimental demonstration, described in a com-

panion article [28], of on-demand vortex generation and manipulation of two oppositely charged vortices to many-vortex distributions, and further characterize the experimental parameters that enable two-vortex generation and manipulation. We refer to this approach as the “chopsticks method.” We consider a highly oblate harmonically trapped BEC that is pierced by multiple blue-detuned laser beams (that play the role of the chopsticks that manipulate the vortices) whose positions and intensities can be dynamically controlled. We examine conditions for which the motion of the laser beams nucleates vortices in such a way that individual vortices are pinned to distinct laser beams during the nucleation process. Our numerical results indicate that on-demand engineering of many-vortex distributions is an experimentally realistic possibility, and open up new directions for the study of vortex dynamics in BECs.

The prototypical case on which our numerical study is based involves the presence of two blue-detuned Gaussian laser beams that pierce a highly oblate BEC. Each laser beam acts as a barrier of maximum potential energy  $U_0$  that is of the same order of magnitude as the BEC chemical potential. Initially, the two beams are stationary and overlap within the BEC. Consider a case where both beams begin to move in the  $y$  direction at a velocity that is significantly lower than the critical speed for vortex *dipole* nucleation. As described in a companion paper [28], the beams push atomic superfluid out of the way, and superfluid fills in the space vacated by the laser beam. Simultaneously, the beams are pulled apart in the  $x$  direction, each beam having equal but opposite  $x$ -velocity component. Then, although the beams are always traveling at a speed well below the critical speed for vortex dipole nucleation, the “holes” (and the specific path they take) created by the laser beams facilitate the formation of two singly quantized vortices of opposite circulation that are simultaneously created and pinned (one per beam). Further slow, adiabatic motion

\*<http://nlds.sdsu.edu>

(below the critical speed) of the laser beams, which serve as vortex optical tweezers, guides the position of the pinned vortices. After using the chopstick beams to transport the vortices to desired locations, they can be released into the BEC to evolve freely by ramping off the laser beams. It is worthwhile to add here that recently an *attractive* impurity has been utilized in a one-dimensional setting, in order to perform similar manipulations for one or more dark solitons [29].

Here we numerically focus on the use of several laser beams to create and manipulate several vortices within the BEC. We show that by moving the laser beams to desired locations and then ramping them off, vortices are released into the BEC and subsequently evolve according to their intervortex dynamics. Since the basic vortex generation process creates two vortices of opposite circulation, neutral vortex charge configurations with equal numbers of vortices of positive and negative circulation can be readily created. However, by driving some of the chopstick beams out of the condensate, nonneutral charge configurations can also be generated. Furthermore, by driving multiple chopstick beams together or onto a separate “repository” laser beam, multiply quantized circulations about a single laser beam can be generated and stored. We confirm that by using either many moving laser beams or by depositing vortices to stationary repository beams and reinitiating the process of creating two pinned vortices with two chopstick beams, arbitrary amounts and configurations of quantized vorticity can be prepared in the system, enabling the examination of a wide array of associated phenomena. An experimental realization of the prototypical scenario considered herein involving two beams is explored in the companion paper [28].

Our discussion is organized as follows. In Sec. II, we briefly discuss the theoretical model that is used for our study, namely the two-dimensional (2D) Gross-Pitaevskii equation (GPE) in the presence of a parabolic trap and a set of localized movable defects. In Sec. III, we present our numerical results. We start with the simplest case of creating two vortices with two chopstick beams, which constitutes our benchmark for quantifying the success of the method, and describe how the vortex generation and trapping process depends on the beam parameters. Subsequently, we demonstrate that the process can be scaled up to neutral configurations of more than two vortices. We then consider the removal of a single vortex from neutral configurations by removing one chopstick beam. For the case of two initial vortices, this allows a single vortex to remain in the condensate at a location that is determined by the remaining beam. More generally, removing a single vortex by driving a beam out of the condensate leaves an imbalanced vortex charge configuration. Although in the present work we will consider imbalances leading to a total charge of  $\pm 1$ , it will be evident that the method can enable arbitrary such imbalances in the system. Finally, we explore a number of variants to the problem. To distill out acoustic energy from these latter vortex configurations, we explore the effect of thermally induced dissipation [30], analyzed for vortices, e.g., in Ref [31–33] (see also references therein). We also present the possibility of depositing large amounts of vorticity of the same charge in a vortex repository. In many cases, we explore the vortex dynamics and distributions that result from ramping off the laser beams. Finally, in Sec. IV, we summarize our findings and discuss directions for future study.

## II. MODEL

We numerically investigate a Bose-Einstein condensate in the presence of a strongly anisotropic trapping potential  $V_{\text{ext}} = \frac{1}{2}m(\omega_x^2 x^2 + \omega_y^2 y^2 + \omega_z^2 z^2)$  with  $\omega_x = \omega_y \equiv \omega_r \ll \omega_z$ . In this case the trapped BEC acquires a nearly planar “pancake” shape. We start from the three-dimensional Gross-Pitaevskii equation

$$i\hbar\partial_t\Psi = -\frac{\hbar^2}{2m}\Delta\Psi + g_{3\text{D}}|\Psi|^2\Psi + V_{\text{ext}}\Psi \quad (1)$$

with  $g_{3\text{D}} = \frac{4\pi\hbar^2 a_s}{m}$ , where  $a_s$  denotes the  $s$ -wave scattering length. The wave function can be factorized into  $\Psi = \Phi(z)\psi(x, y, t)$ , where  $\Phi(z)$  is the ground state of the respective harmonic oscillator,  $\Phi(z) = \left(\frac{m\omega_z}{\pi\hbar}\right)^{1/4} e^{-m\omega_z \frac{z^2}{2\hbar}}$ , and  $\psi(x, y, t)$  is normalized to the number of atoms. Multiplying Eq. (1) by  $\Phi^*(z)$  and integrating over all  $z$  yields the 2D GPE:

$$i\hbar\partial_t\psi = -\frac{\hbar^2}{2m}\Delta\psi + g_{2\text{D}}|\psi|^2\psi + V_{\text{ext}}(x, y, z=0)\psi. \quad (2)$$

Here, we have introduced the 2D interaction parameter  $g_{2\text{D}} = g_{3\text{D}}/(\sqrt{2\pi}a_z)$  and the harmonic oscillator length  $a_z = \sqrt{\hbar/m\omega_z}$ .

We nondimensionalize the 2D GPE by setting  $\tilde{t} = t\omega_z$ ,  $(\tilde{x}, \tilde{y}) = (x, y)/a_z$ , and  $\tilde{\psi} = a_z\psi$ . The dimensionless 2D GPE then becomes

$$i\tilde{\psi}_{\tilde{t}} + \frac{1}{2}(\tilde{\psi}_{\tilde{x}\tilde{x}} + \tilde{\psi}_{\tilde{y}\tilde{y}}) - g|\tilde{\psi}|^2\tilde{\psi} - V\tilde{\psi} = 0, \quad (3)$$

where  $g = 4\pi a_s/(\sqrt{2\pi}a_z)$  and  $V = \frac{\Omega^2}{2}(\tilde{x}^2 + \tilde{y}^2)$ , where the effective (2D) harmonic trapping frequency is  $\Omega = \omega_r/\omega_z$ . Further letting  $u = \sqrt{g}\tilde{\psi}$ , and dropping all tildes hereafter for notational simplification, the 2D GPE for the case of repulsive interatomic interactions then becomes

$$iu_t + \frac{1}{2}(u_{xx} + u_{yy}) - |u|^2u - Vu = 0. \quad (4)$$

In the presence of  $N$  Gaussian laser beams of identical  $1/e^2$  radii  $\sigma$  (a dimensionless length, measured in units of  $a_z$ ), the external effective (2D) potential is given by the following combination of harmonic trapping and the laser beams:

$$V(x, y, t) = \frac{\Omega^2}{2}(x^2 + y^2) + \sum_{j=1}^N U_{0,j} e^{-\frac{(x-x_j)^2 + (y-y_j)^2}{\sigma^2}}, \quad (5)$$

where, for the  $j$ th laser beam,  $U_{0,j}$  and  $(x_j(t), y_j(t))$  are, respectively, the time-dependent height of the light-induced barrier measured in units of  $\hbar\omega_z$  and its position measured from the trap center in units of  $a_z$ .

For ease of evaluation of the experimental possibility of utilizing our vortex generation and manipulation methods in the discussion below, we define and utilize a *dimensional* measure of the full width at half maximum of the chopstick beams as  $b_w = a_z\sqrt{2\ln(2)}\sigma$ . The beam height  $U_{0,j}$  for each beam is given in terms of the chemical potential  $\mu$  measured in units of  $\hbar\omega_z$ . Furthermore, we specify all velocities in terms of the maximum sound speed

$$c = \frac{2\hbar}{m}\sqrt{\pi a_s n_{\text{max}}}, \quad (6)$$

where  $n_{\max}$  is the maximum of the three-dimensional atomic density (usually attained at the center of the parabolic trapping)

$$n_{\max} = \left(\frac{m\omega_z}{\pi\hbar}\right)^{1/2} \max(|u|^2) / \left(\frac{4\pi a_s a_z}{\sqrt{2\pi}}\right). \quad (7)$$

Our procedure is conceptually similar to that of the companion article [28], where blue-detuned laser beams are used in order to produce repulsive barriers that generate and then dynamically manipulate vortices inside the BEC. We specify parameters used in the calculations, and present the results of our numerical simulations using those parameters.

As mentioned previously, in recent years a significant consideration in connection to vortices concerns their dynamics in the presence of thermally induced dissipation; see, e.g., Refs. [30–34] for which the system is described by the dissipative Gross-Pitaevskii equation (dGPE)

$$(i - \gamma)u_t + \frac{1}{2}(u_{xx} + u_{yy}) - |u|^2u - (V - \mu)u = 0, \quad (8)$$

where  $\gamma$  is a dimensionless, phenomenological, damping constant—depending on the temperature of the condensate; see, for instance, Ref. [35]—and  $\mu$  is the (adimensional) chemical potential that the BEC equilibrates to for the given temperature. As we show below, considering dissipation in our system not only corresponds to a more realistic experimental scenario, but it helps to remove vortices from the periphery of the BEC cloud as dissipation induces them to spiral outwards.

### III. NUMERICAL RESULTS

The initial condition for our evolutionary dynamics is obtained by a 2D fixed point iteration (a Newton’s method) in order to identify the ground state of the system in the presence of an even number of beams, ranging from two to eight. This state is devoid of vortices. Subsequently, we compute the time evolution using a variable-order Adams PECE algorithm, of the type originally elaborated in Ref. [36].

Although our findings can be straightforwardly generalized to different trapping and atomic gas parameters, for concreteness within our pancake-shaped geometry, we choose parameter values consistent with the experiments of the companion article [28]. Namely, we choose  $\omega_r = 2\pi \times 2$  Hz,  $\omega_z = 2\pi \times 90$  Hz, and  $a_s = 5.3$  nm corresponding to  $^{87}\text{Rb}$  [48]. We examine a range of chemical potentials, and indicate this value of  $\mu$  for each case study. These parameters correspond to dimensionless times measured in units of 1.77 ms.

#### A. Neutral vortex configurations

First we discuss the generic example of the creation and trapping of a pair of oppositely charged vortices that can later be used as a building block for the generation of a larger distribution of an even number of vortices, with equal numbers of positively and negatively charged trapped vortices. Two beams of equal waist and height are initially located at the same position and are subsequently moved with the same speed under a suitable angle to two different final positions. For a given value of the beam size  $b_w$ , there is a range of suitable values of the beam velocity, exceeding a (lower) critical value but much less than the speed of sound, for which the flow around the beams results in the generation and pinning of

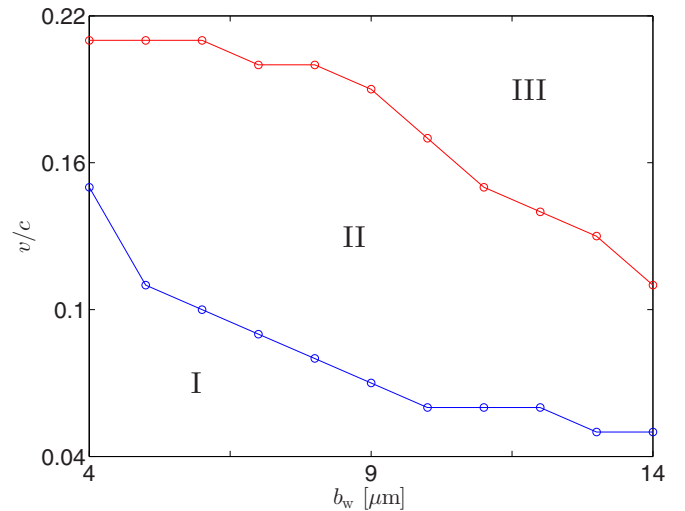


FIG. 1. Regions of successful and unsuccessful vortex generation and trapping as a function of the beam width  $b_w$  and the scaled chopsticks speed  $v/c$ . The chemical potential corresponds to  $\mu = 1.5$  and the beam height is  $2\mu$ . Both beams are initially situated at  $(0, -20)$   $\mu\text{m}$  and moved diagonally on straight lines with the corresponding velocity to their final positions at  $(\pm 10, 0)$   $\mu\text{m}$ . Region I: The velocity of the chopsticks is too small and vortices are not created. Region II: Two vortices of opposite charge are created, successfully trapped, and dragged along with the laser beams. Region III: The velocity of the laser beams is too large, resulting in the vortices being lost from their respective beams and remaining behind the beams. For beamwidths approximately smaller than  $b_w = 4$   $\mu\text{m}$  no vortex trapping is supported: any vortices created are immediately lost from the beams. Movies showing the full time evolution exemplary for each of the three regimes (and for each of the following figures) can be found at <http://nonlinear.sdsu.edu/~carreter/Chopsticks.html>.

two vortices with opposite charge. If the velocity is chosen to be higher than this range, vortices are created but cannot remain trapped by their respective beams. These vortices start lagging behind their respective beams and finally are released from the trapping action of the chopstick beams. The vortices may then annihilate one another. Given that this is a prototypical *benchmark* scenario, in Fig. 1 we display regions of successful and unsuccessful vortex generation and stable trapping and manipulation, for various beamwidths  $b_w$  and beam speed  $v/c$  [measured in units of the maximum speed of sound; see Eq. (6)] for an experimentally realistic chemical potential  $\mu = 1.5$ , which corresponds to  $\sim 4.4 \times 10^5$  atoms comprising the BEC for the parameters given previously, a radial Thomas-Fermi BEC radius of  $\sim 87$   $\mu\text{m}$ , and a BEC healing length of  $\sim 0.64$   $\mu\text{m}$ . The waist of the beams should be large enough to support the existence and trapping of the vortices. We find that for the BEC parameters used in our study, with  $\mu \sim 1.5$ , the beamwidth approximately has to exceed 4  $\mu\text{m}$ . For beamwidths below this value, the vortices created are immediately expelled from the trapping beams [37]. We have used throughout this study a beam height twice as large as the BEC chemical potential ( $U_{0,j} = 2\mu$ ). However, we have checked that for lower beam heights between  $U_{0,j} = \mu$  and  $U_{0,j} = 2\mu$ , vortex nucleation is still successful for beamwidths approximately larger than 4  $\mu\text{m}$ .

We now examine the trajectories of two oppositely charged vortices that result from turning off the chopstick beams, in the case of typical symmetric and asymmetric configurations of the vortices [9]. We choose a value of  $\mu = 1.5$  for the chemical potential, a beam waist  $b_w = 6 \mu\text{m}$ , and a beam height  $U_{0,j} = 2\mu$ . It is worth mentioning at this stage that lower values of the chemical potential resulted in large (density modulation) disturbances as the chopsticks move through the condensate, especially if more than two beams are present; on the other hand, the case of larger values of the chemical potential is more difficult to track numerically as the vortex width becomes relatively small compared to the numerical domain and thus a large numerical grid is necessary. Therefore, for larger numbers of trapped vortices, discussed later, it is necessary to increase the value of  $\mu$  at the expense of more intensive numerics. The typical generation of a symmetric vortex configuration is shown in Fig. 2. After the vortices have been created and have reached the desired symmetric final positions ( $\pm 10, 0$ )  $\mu\text{m}$  the beams are adiabatically and linearly ramped down to release the vortices to undergo free (i.e., uninhibited by the presence of the chopstick beams) time evolution. As a result, the released vortices exhibit the typical dynamical features of a vortex dipole configuration [9,38]. This is illustrated in Fig. 3(a) for the symmetric case of Fig. 2. Figure 4 shows a similar example to the one depicted in Fig. 2 but for an asymmetric motion of the chopsticks. In this case, one laser beam is kept fixed after  $t = 110$  at (10,0)  $\mu\text{m}$  while the other beam is moved further until  $t = 200$  where both beams are kept fixed and ramped down. This procedure seeds an asymmetric configuration that, after removal of the chopsticks, evolves in the typical epitrochoidal trajectories for asymmetric vortex dipoles [9,38] as shown in Fig. 3(b).

Next, we investigate the possibilities to create larger, even numbers of vortices in a neutral configuration with four,

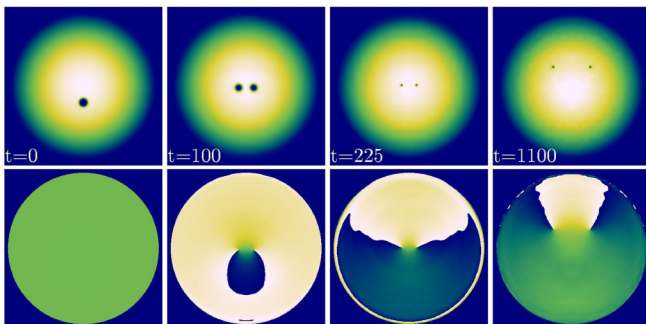


FIG. 2. Controlled generation of a vortex dipole for  $\mu = 1.5$ . Throughout this paper the upper row shows the atomic density in false color (white corresponds to highest densities, blue to lowest) while the lower row displays the phase (blue to white corresponds to phases from 0 to  $2\pi$ ) at the times indicated in the legend. A pair of beams with  $b_w = 6 \mu\text{m}$  and beam height  $U_{0,j} = 2\mu$  initially ( $t = 0$ ) placed at  $(0, -20) \mu\text{m}$  are moved within  $\Delta t = 110$  to  $(\pm 10, 0) \mu\text{m}$ . The process nucleates a vortex dipole that is dragged along to the desired location. From  $t = 110$  to  $t = 210$  the beams are linearly ramped down to release the vortices to the free time evolution where the vortices start the typical motion of a symmetric dipole pair. The numerics for  $\mu = 1.5$  are run on  $749 \times 749$  grid points. The resulting spatial discretization  $dx = 0.23$  guarantees the existence of about 10 grid points within the vortex profile.

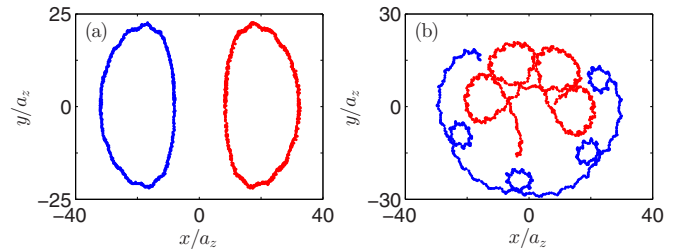


FIG. 3. (a) Vortex trajectories for the symmetric vortex configuration from Fig. 2 displayed from the release of vortices at  $t = 210$  up to  $t = 4000$ . (b) Vortex trajectories for the asymmetric configuration of Fig. 4 from release of vortices up to  $t = 16000$ . Blue [(a) left and (b) outer] and red [(a) right and (b) inner] curves represent the trajectories for each vortex.

six, and eight vortices. The idea is to start with two, three, or four pairs of overlapping chopstick beams close to the center of the BEC and use the same methodology as above to create vortices from each beam pair with the same protocol as described above. Doing so, each chopstick nucleates and moves an independent vortex that might be placed in a desired location. The beams then are kept fixed at their final destination and subsequently linearly and adiabatically ramped down to release the vortices that in turn are free to evolve without the chopsticks being present. Figure 5 shows that this methodology is indeed feasible for controllably creating, moving, and releasing configurations bearing four, six, and eight vortices. In principle, this method can be straightforwardly generalized to even larger numbers of vortices as long as there is enough room within the BEC to move the chopstick beams. As can be observed from the last density distributions, the motion and removal (ramping down) of multiple chopsticks has a significant perturbative effect on the background density. In fact, if the disturbances to the condensate are considered to be too strong, it would be advantageous to increase the value of the chemical potential in order to diminish the role of interference of the resulting sound waves. For this purpose, in our examples with multiple chopsticks we choose a slightly larger value of the chemical potential (when compared to the previous results with a single chopstick pair) of  $\mu = 2$ . In view

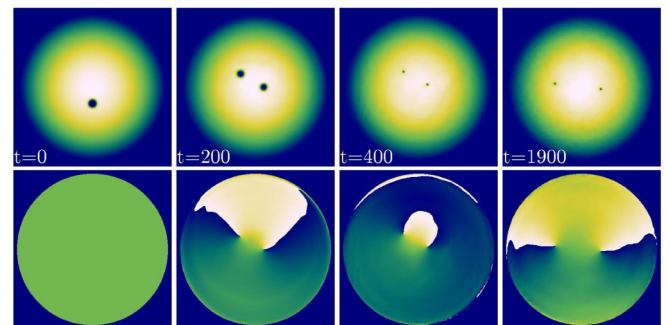


FIG. 4. Similar to Fig. 2 but for an asymmetric vortex configuration. While one beam is kept fixed after  $t = 110$  at  $(10, 0) \mu\text{m}$ , the other beam is moved further until  $t = 200$ . Then both beams are kept fixed in this asymmetric configuration and are linearly ramped down within  $\Delta t = 100$ . As a result, asymmetric vortex dipole dynamics arises past the ramp-down time.

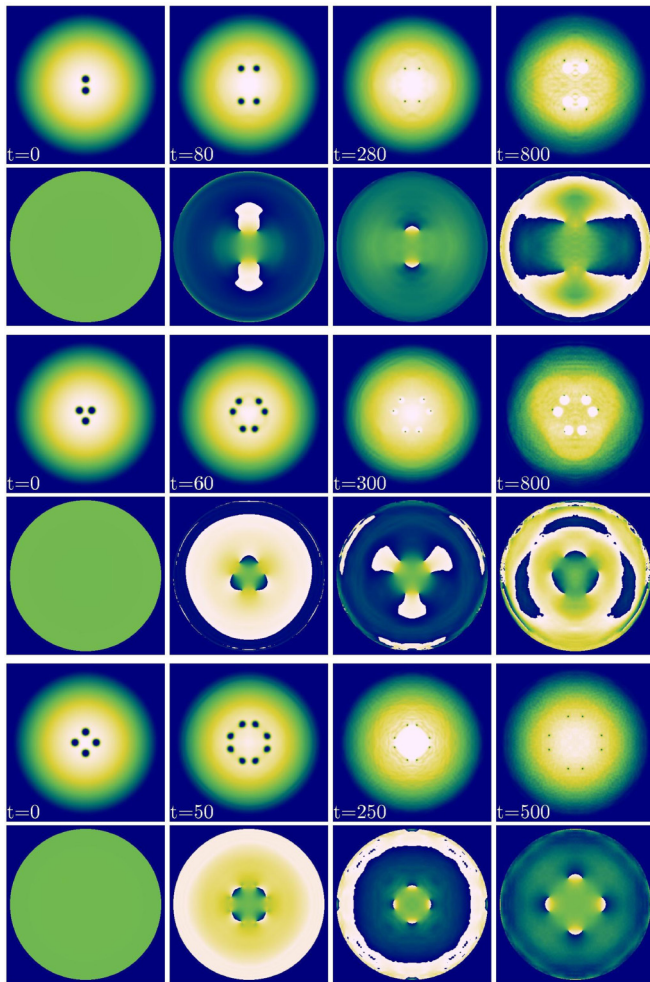


FIG. 5. Controlled generation of four, six, and eight vortices. Chosen parameters are chemical potential  $\mu = 2$ , beam heights  $2\mu$ , and beam widths  $b_w = 6 \mu\text{m}$ . Upper set of panels: Two pairs of beams initially located at  $(0, \pm 8) \mu\text{m}$  are moved outward with  $v/c = 0.123$  until  $t = 80$ , then their positions are kept fixed. From  $t = 80$  until  $t = 280$  the beams are linearly ramped down, the vortices are finally released, and the time evolution is monitored. Middle panel: Similar but for 3 pairs of beams initially located symmetrically at a distance of  $10 \mu\text{m}$  from the origin with linear ramp-down from  $t = 70$  until  $t = 270$ . Lower panel: Similar but for 4 pairs of beams initially symmetrically located at a distance of  $15 \mu\text{m}$  from the origin and moved at a speed  $v/c = 0.15$  and linearly ramped down from  $t = 50$  until  $t = 250$ .

of the disturbances created by a larger number of beams, we found that starting close to the center of the BEC and moving the beams outward is advantageous in comparison to starting further outwards and moving the beams inward.

### B. Nonneutral configurations

We now consider creating an odd number of vortices with a charge imbalance of one, such that there is one more or one fewer positively charged vortex compared with negatively charged vortices. To create such a nonneutral distribution in a controllable and repeatable manner we start by creating a neutral configuration as discussed in the previous section

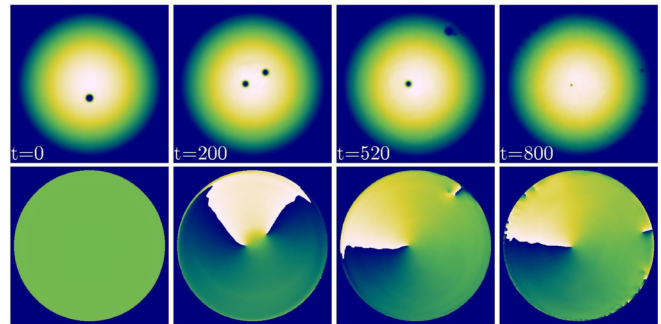


FIG. 6. Controlled generation of a single vortex for  $\mu = 2$ , beam height  $2\mu$ , and beamwidth  $b_w = 6 \mu\text{m}$ . The initial pair of beams located at  $(0, -20) \mu\text{m}$  is moved with  $v/c = 0.106$  to  $(\pm 10, 0) \mu\text{m}$ . One beam is then kept fixed at this position while the other one is moved further outwards, dragging the associated vortex with it. At  $t = 500$  the former beam is ramped linearly down within  $\Delta t = 100$  to release the single vortex close to the condensate center. The chosen grid size for this case is  $749 \times 749$  resulting in a spatial discretization with spacing  $dx = 0.26$ .

and then take one vortex out of the condensate. We first demonstrate this procedure starting with a pair of oppositely charged vortices, removing one of the vortices, and leaving a single vortex that can then be repositioned at will. The creation of a larger nonneutral configuration of vortices follows a similar principle.

Figure 6 illustrates the ability to create a single vortex. First the protocol follows the generation of two vortices as in Fig. 2. When the beams have reached  $(\pm 10, 0) \mu\text{m}$ , one of the beams is kept stationary at its position while the other beam is moved further towards the edge of the condensate, dragging the trapped vortex with it. Ideally, the vortex would be dragged all the way out of the condensate. However, shortly before reaching the edge of the condensate the vortex detaches from the beam and this edge vortex starts circulating indefinitely around the condensate (see Fig. 6 where the vortex is barely visible in the last two density snapshots, but is clearly visible in the corresponding phase profile). This type of “detachment” is a general issue that is encountered when trying to “rid” the configuration of individual vortices by moving one of the beams out of the BEC in a direction that is normal to the edge of the BEC. A number of pointers about how to bypass this issue, most notably adjustments to the beam trajectory, and relying on the dissipation stemming from thermal excitations, is discussed below. As soon as the outgoing beam has reached the edge of the condensate the first beam is linearly and adiabatically ramped down to release the remaining single vortex to undergo free time evolution.

While it is advantageous to reduce the beam velocity when dragging the vortex out to allow the vortex to follow the beam trajectory closer to the edge of the condensate (at the cost of larger time scales), typically in our observations it is not sufficient to drag the vortex all the way out of the BEC. This is due to the fact that the density becomes small at the condensate edge and thus the (density) contrast created by the laser beam close to this edge is too small to pin or drag a vortex. Nonetheless, we have found that the presence of dissipation (typically present in all BEC experiments),

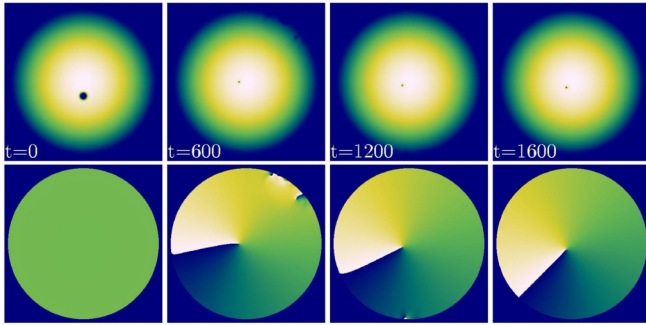


FIG. 7. Similar to Fig. 6 but in the presence of dissipation, as described by Eq. (8) with  $\gamma = 2 \times 10^{-2}$ .

as described by Eq. (8), can resolve this issue. Figure 7 depicts the results corresponding to Fig. 6 with the addition of dissipation with  $\gamma = 2 \times 10^{-2}$ . As is evident from the figure, at  $t = 1200$  the edge vortex is already very close to the edge of the condensate (as is visible in the phase profile) and has completely left the condensate by  $t = 1600$ . Figure 8 shows a similar case but for the experimentally more realistic value  $\gamma = 2 \times 10^{-3}$ ; see the relevant discussion in Ref. [33], as well as in earlier works on coherent structures such as dark solitons in Ref. [39]. In this case, the vortex is still visible at  $t = 8000$  and has completely left the condensate at  $t = 12000$ . We find the time scale for expelling the edge vortex from the condensate—with a starting point at about  $t = 600$  where the dragging beam has reached the edge of the condensate—to be approximately a factor ten times larger than that for  $\gamma = 2 \times 10^{-2}$ . As the physical picture is qualitatively the same but the (computational) time scales are considerably shorter in the following we will always opt to use the value  $\gamma = 2 \times 10^{-2}$  to obtain results in the presence of dissipation. It is relevant to mention at this stage that the value of  $\gamma$  depends on the temperature of the condensate. For instance, for a BEC of sodium it was recently found that the relationship between the phenomenological damping coefficient and the temperature was monotonic (larger coefficient corresponding to higher temperatures) [35]. Under these very recent experimental conditions, values of  $\gamma$  such as  $2 \times 10^{-3}$  lie at the edge of the accessible region of temperatures.

A more efficient protocol to drag a vortex out of the BEC relies on adjusting the laser beam path such that its trajectory becomes more azimuthal as the beam gets closer to the edge

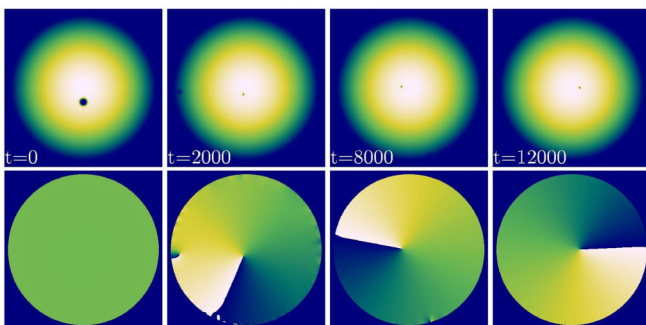


FIG. 8. Similar to Fig. 7 but in the presence of a more realistic dissipation value of  $\gamma = 2 \times 10^{-3}$ .

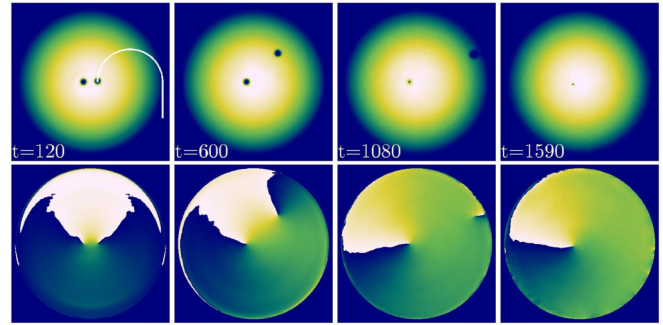


FIG. 9. Improved protocol to create a single vortex. Same as Fig. 6 but with a circular trajectory (as indicated by the white line in the left panel) instead of a straight line to drag the vortex out of the condensate. Additionally, the velocity of the dragging beam is reduced by 50% after  $t = 110$ . At  $t = 1000$ , when the latter beam starts to leave the condensate, the other beam is ramped down linearly within  $\Delta t = 100$ .

of the BEC and thus mimicking the natural tendency of the vortex to precess about the trap center. Figure 9 depicts this improved protocol where one of the beams is moved on a circular path of diameter equal to the Thomas-Fermi radius (see white line) such that it leaves the condensate tangentially. Additionally, the velocity of the dragging beam is reduced by 50% after  $t = 110$ . This results in the successful creation of a single vortex at  $t = 1620$  as the second vortex seems to be completely removed from the BEC (it is not visible in the density nor in the phase plot).

For the generation of three, five, or seven vortices with a charge imbalance of one, the idea is the same: start with a neutral configuration with four, six, or eight vortices (see Fig. 5) and displace one beam outward with the aim of removing a single vortex from the neutral configuration. More specifically, after an even number of vortices is created, all but one of the beams then are kept stationary at their respective locations while the remaining beam is moved further outward to ideally drag the trapped vortex all the way out of the condensate. This is followed by linearly ramping down the other beams and releasing the vortex configuration in order for it to perform free (i.e., unaffected by the beams beyond this time) time evolution. The results for this proposed methodology are displayed in Fig. 10. The case for initially four (and subsequently three) vortices is depicted in the top two panels in Fig. 10. This case is more successful than for the creation of a single vortex; i.e., here the remaining vortex has nearly vanished in the background. The case corresponding to initially six (and subsequently five) vortices is depicted in the middle rows of panels in Fig. 10. In this case, the edge vortex is still visible at  $t = 1200$  but cannot be distinguished from the background at  $t = 1600$ . Finally, the bottom rows of panels in Fig. 10 illustrate the results for initially eight (and subsequently seven) vortices. This case example is again fairly successful in the sense that a potential edge vortex cannot be distinguished from the background.

### C. Comparison with vortex imprinting method

The dynamics of vortices can also be explored by imprinting vortex solutions onto the ground-state BEC in the presence

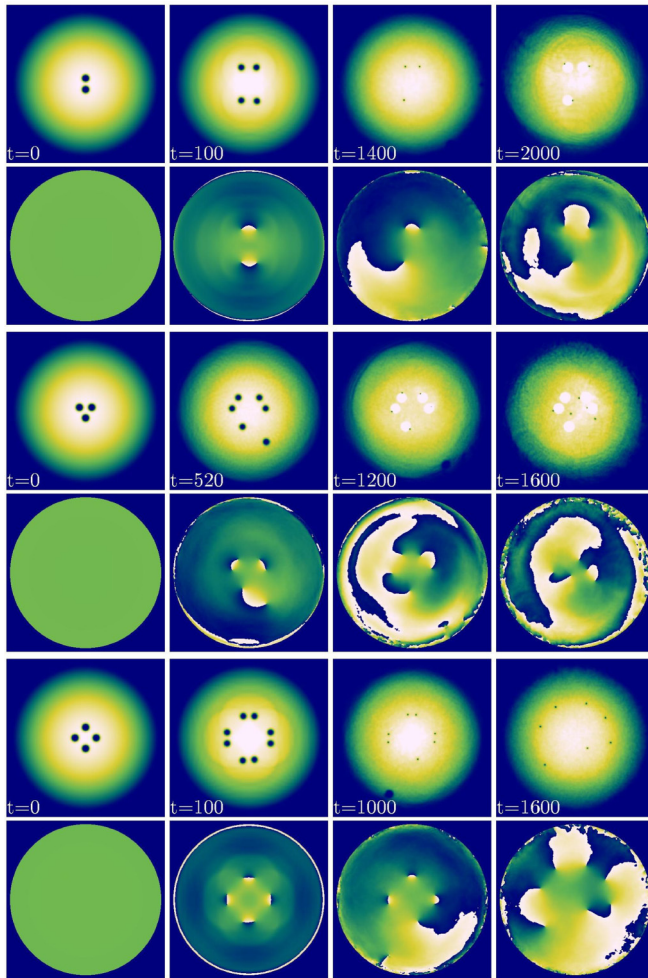


FIG. 10. Controlled generation of an odd number of three to seven vortices for the same parameters and initial configurations as in Fig. 5. Upper rows: At  $t = 80$ , three beams are kept fixed, while beam number four is moved further outwards dragging one vortex out of the condensate. The beam velocity is reduced to 25% of its original value. After linearly ramping down from  $t = 1200$  to  $t = 1400$  the other vortices are released from their beams. Middle rows: Similar but for six vortices stemming from three pairs of beams. Five beams are kept fixed at  $t = 65$  and linearly ramped down from  $t = 600$  to  $t = 800$ , leading to a five-vortex configuration, while the other is moved out of the condensate, again with reduced speed of 25% of the original value. Bottom rows: Similar to the previous cases but for four pairs of beams. Seven beams are kept fixed at  $t = 75$  and linearly ramped down from  $t = 800$  to  $t = 1000$  while one vortex is dragged all the way out of the condensate, endowing the system with a configuration of seven vortices of alternating charge.

of only the harmonic confinement. Such a technique has been used successfully in generating coherent structures [40], although it should be noted that typically in these experiments only a phase imprinting is induced. The latter necessitates the “morphing” of the density around the imprinting spot into a vortex profile, a process which, in turn, generates considerable sound wave emission clearly visible in some of the case examples of Refs. [40]. Here, when we refer to imprinting, we more accurately mean both phase and density engineering, or “implanting” a vortex in the system, namely imprinting the

phase, concurrently with modulating the density in order to produce an “as nearly exact as possible” vortex wave form in the system. While the latter scenario is quite idealized and not straightforwardly achievable practically in the laboratory, our aim is to compare the dynamics of our produced vortices via the chopsticks method (containing the density modulations induced by the light beams, etc.) to “target” vortex dynamics for a similar set of initial vortex locations.

In the following we compare the time evolution that is initialized by the chopsticks method and compare it with the results obtained for the vortex implanting method. It should be stressed that while the chopsticks method generates (sometimes large) sound waves in the condensate as well as allowing vortices to move prior to fully ramping off the laser beams, the implanting method generates the most pristine setting with minimal sound creation and nearly “pure” vortex dynamics. Note that this is a numerical comparison only, as there have not been any demonstrations of phase engineering and imprinting of arbitrary vortex distributions into a BEC. We choose the case of three vortices, as displayed in the top rows of Fig. 11. To initialize the vortex implanting method we determine the positions and charge of the three vortices (resulting from two sets of split beams as explained in the previous subsection) at  $t = 1400$ . The ground-state solution of the BEC is then multiplied with the corresponding (normalized) vortex solutions (obtained for a homogeneous background BEC) at the desired locations (this is the “implanting” part). Figure 11 clearly shows that the two methods generate a nontrivially differing time evolution. While the qualitative structure of the vortex positioning and trajectories when using the chopsticks has been found to follow that of the “implanted” vortex configuration with the same initial vortex positions, the density modulations induced by the vortex generating beams definitely affect the precise aspects of the vortex dynamics.

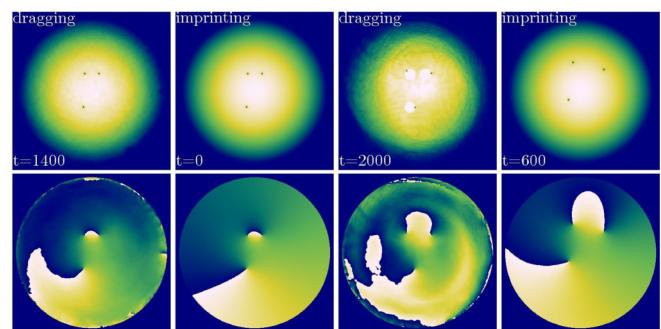


FIG. 11. Comparison of the chopsticks protocol and the vortex implanting method for the example of the three vortices from Fig. 10 for the configuration at  $t = 1400$  after releasing the vortices from the beams (first column). For the vortex implanting method the time evolution is initialized by a wave function with two negatively charged vortices of charge located at  $(-10.025, -20.075)$  and  $(9.25, 21.5)$  and one positively charged vortex located at  $(-8.45, 21.5)$  (second column). Observable differences in the time evolution can be observed in comparison to the time evolution generated by the chopsticks method and the vortex implanting method’s dynamics (columns three and four, respectively) due to the generation of sound waves in the former method.

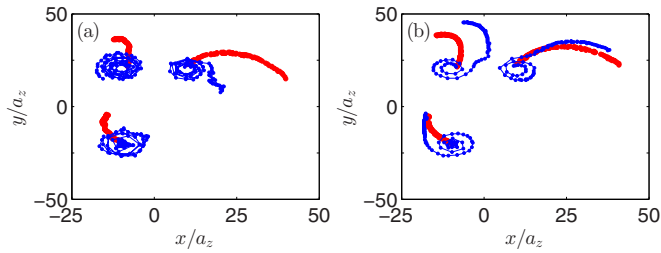


FIG. 12. Vortex trajectories corresponding to the cases depicted in (a) Fig. 11 and (b) Fig. 13. The orbits in blue correspond to the chopsticks method while the red orbits correspond to the implanting method.

The comparison of the corresponding trajectories using both methods is depicted in Fig. 12(a).

Next, and for reasons of completeness, we investigate the influence of dissipation on both cases. While the presence of dissipation with  $\gamma = 2 \times 10^{-2}$  again helps to expel the edge vortex from the condensate that is visible at  $t = 1400$  (and barely visible at  $t = 2000$ ) for the vortex dragging method it does not have a big influence on the motion of the other three vortices closer to the BEC center. Also for the vortex implanting case the influence is negligible; cf. Fig. 13. Hence, unfortunately, in this case the presence of thermal excitations does not considerably alleviate this discrepancy. The comparison of the corresponding trajectories using both methods is depicted in Fig. 12(b).

#### D. Repositories

Lastly, we explore the possibility of depositing several vortices in so-called repository beams. The latter can be important for various reasons in the form of persistent currents [37,41], but also towards the monitoring of dynamics of large vortex clusters aggregating with a single sign of vorticity, so-called Onsager-Kraichnan condensates, also thermodynamically representing negative temperature states; see, e.g., the recent analysis of Ref. [42].

As an example, we investigate a configuration where two stationary repository beams with large beam waist are located in the BEC; cf. Fig. 14. The idea is to create one pair of oppositely charged vortices after another and deposit the positively charged vortices in one of the repositories while the negatively

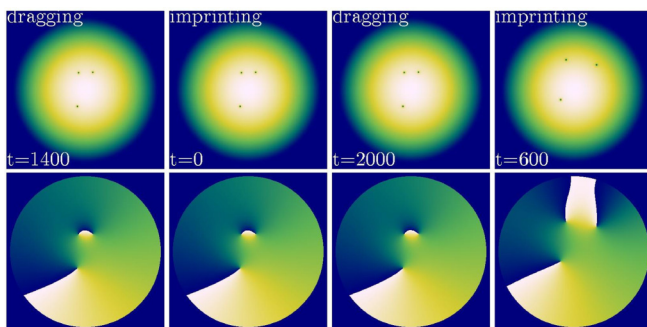


FIG. 13. Same as Fig. 11 but in the presence of dissipation with  $\gamma = 2 \times 10^{-2}$ .

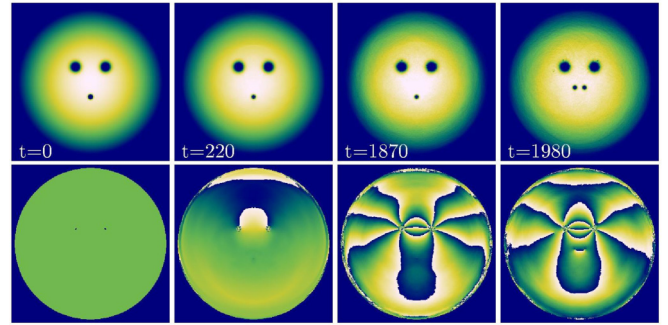


FIG. 14. Principle of repository beams: Two stationary large beams with  $b_w = 15 \mu\text{m}$  and beam height  $2\mu$  serve as repository beams to collect vortices of equal charge. Vortices are created in oppositely charged pairs by ramping up two chopstick beams with  $b_w = 6 \mu\text{m}$  at  $(0, -30) \mu\text{m}$  (at  $t = 0$  they are already present) and by moving the beams to the pinning sites at  $(\pm 30, 30) \mu\text{m}$ . When the beams reach the pinning sites they are ramped down while new chopstick beams are ramped up at  $(0, -30) \mu\text{m}$ . At  $t = 220$  one vortex is present in each repository beam; at  $t = 1870$  seven vortices are present in each pinning site. If a certain critical number of vortices per pinning site is exceeded vortices start leaking out of the repository beams; cf. panel for  $t = 1980$  where a vortex has been expelled from the repository beam. For this value of the chemical potential ( $\mu = 4$ ), the grid size is increased to  $1199 \times 1199$ , and  $dx = 0.23$ .

charged vortices are deposited in the other repository beam. In this way, persistent currents can be obtained [41]. The vortex generation portion of the sequence follows the principle illustrated in Fig. 2. When the chopsticks reach the repository beams their position is kept fixed and they are linearly ramped down while a new chopsticks pair is linearly ramped up and another pair of vortices is created and dragged to the repository beams. This procedure can be repeated until a critical number of vortices is trapped in each repository beam. As soon as a certain number of vortices—depending on the size of the repository beam—is exceeded, vortices start leaking out of the repositories. A natural constraint in that regard is that the repository beamwidth should be larger than the product of the number of vortices times their corresponding length scale, i.e., the healing length of the BEC.

To create a large number of vortices within this procedure with as little disturbance of the condensate as possible, it is advantageous to use a larger chemical potential. In the following, we choose  $\mu = 4$ . The size of the chopstick beams is again  $b_w = 6 \mu\text{m}$ . In Fig. 14 we display results for repository beams with  $b_w = 15 \mu\text{m}$ . The time evolution is initialized by using the stationary state with two chopstick beams present at  $(0, -30) \mu\text{m}$  and repository beams located at  $(\pm 30, 30) \mu\text{m}$ . For a duration  $\Delta t = 233$  the chopstick beams are moved towards  $(\pm 30, 30) \mu\text{m}$ , creating and dragging the first pair of vortices with them. At the position of the repository beams the chopstick beams are linearly ramped down within  $\Delta t = 100$  and the respective vortices are consequently deposited in the repository beam. While the old chopstick beams are ramped down a new chopsticks pair is linearly ramped up at the same initial position as the former, again within  $\Delta t = 100$ . Then the whole procedure is repeated and the second vortex dipole pair is created, dragged along, and deposited, respectively, within

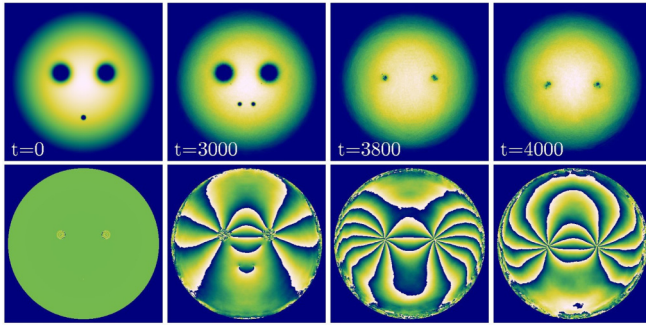


FIG. 15. Similar to Fig. 14 but with larger chemical potential  $\mu = 5$  and larger repository beams with  $b_w = 30 \mu\text{m}$ . In this way ten vortices can be trapped per repository beam. Within  $\Delta t = 265$  the dragging beams are moved toward the repositories and ramped up/down within  $\Delta t = 100$ . At  $t = 3550$ , the repository beams are linearly ramped down within  $\Delta t = 100$  to release the vortices towards subsequent free time evolution. A slight amount of sound emission is present in the dynamics due to the density modulations imposed by the repository beams. For this value of the chemical potential ( $\mu = 5$ ) the grid size is further increased to  $1499 \times 1499$ , resulting in  $dx = 0.21$ .

the repository beams. For the chosen size of the repository beams seven vortices can be placed into each beam. After this critical number has been reached, vortices start leaking out of the repository beams. At  $t = 1980$  the first vortex has been expelled from the repository beam.

To accommodate even more vortices within the repositories, we increase the chemical potential to  $\mu = 5$  and the size of the repository beams to  $30 \mu\text{m}$ . For these parameters ten vortices can be deposited in each repository; cf. Fig. 15. Next, both the chopstick and the repository beams are linearly ramped down within  $\Delta t = 100$  to release the vortices towards free time evolution. Figure 16 shows the same protocol as in Fig. 15 but in the presence of dissipation with  $\gamma = 2 \times 10^{-2}$ . It can be seen that the introduction of dissipation is, in fact, beneficial: the disturbances (relevant sound waves) to the atomic cloud due to the density modulations induced by the repositories, which can be seen in Fig. 15, are considerably smoothed out in the dissipative case.

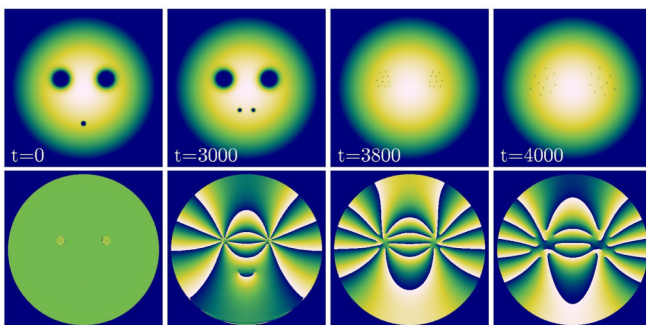


FIG. 16. Same as Fig. 15 but in the presence of dissipation with  $\gamma = 2 \times 10^{-2}$ . Notice that the sound waves have been chiefly expelled from the BEC, enabling a more pristine monitoring of the vortex dynamics.

This specific configuration with two repository beams can easily be modified to other interesting configurations. Note that a repository beam sitting on the edge of the condensate can serve as a location to trap edge vortices that can arise when a vortex is supposed to be taken out of the condensate as in Fig. 6 in a reproducible manner. However, note that our results demonstrate that the presence of dissipation helps to get rid of the edge vortices while the vortices closer to the center are less affected by the latter.

#### IV. CONCLUSIONS AND FUTURE CHALLENGES

In the present work, we have numerically explored a mechanism that enables the production and manipulation of multiple quantized vortices, essentially at will, inside an atomic Bose-Einstein condensate. The use of lasers as vortex “optical tweezers” in a judicious manner, so as to gradually create the phase profile associated with a pair of oppositely charged vortices, as well as to pin vorticity and create persistent current, enabled us to locate vortices at various positions within the BEC by moving the laser beams. We were subsequently able to transfer these vortices at will, including moving them outside the BEC or positioning them within a repository beam. Repeating the process either with multiple optical beams or after the delivery of the first pair to the repository beams, starting the process anew, we were able to produce arbitrary neutral and nonneutral vortex distributions. Naturally, the process has a number of limitations, such as the emergence of density modulations due to the carrying beams (which also to some extent affect the vortex motions), or in some cases the difficulty of carrying individual vortices outside the condensate (due to the so-called “detachment” from the beam in regions of low density near the condensate rims). With respect to most of these aspects, the contribution of thermal fluctuations in the context of the so-called dissipative Gross-Pitaevskii equation is beneficial, enabling the outward motion of vortices and also the partial reduction of sound waves. The method is also generally limited by the number of laser beams of finite width that can be located and moved within a BEC of finite radius.

This technique creates a broad set of possibilities that are quite worthwhile for subsequent experimental and further numerical exploration. As far as we know, no other technique available in the literature is as versatile towards creating/engineering multiple vortices while selecting their charge and position distributions at will. Constructing and understanding the dynamics of such vortices and vortex clusters [43,44], especially in the context of anisotropy where they can be robust, e.g., in collinear states [45,46], and exploring more systematically their stability is now a tractable and experimentally realizable topic. Further studies oriented towards devising methods of decreasing the generation or effects of residual sound waves so as to enable a more direct engineering of free-vortex states and initialization and study of vortex dynamics would certainly be desirable. This would be especially important towards being able to use the particle picture developed for vortices (as well as for dark solitons in 1D and vortex rings in 3D) to understand subsequent vortex dynamics. However, it should be highlighted here that our results are only a first step towards the creation of the relevant vortex patterns, while a more systematic treatment

of the thermal density and phase fluctuations is worthwhile to consider in future work; cf. e.g. [47]. Finally, extending these types of methods to higher dimensional BECs in three dimensions in the case of vortex lines and vortex rings would be of particular interest in its own right.

#### ACKNOWLEDGMENTS

We would like to thank Q.-Y. Chen and Logan Richardson for discussions and numerical assistance during the early stages of this project. B.G. acknowledges support from the European Union through FP7-PEOPLE-2013-IRSES Grant No. 605096. P.G.K. acknowledges support from the National

Science Foundation under Grant No. DMS-1312856, from the European Union through FP7-PEOPLE-2013-IRSES Grant No. 605096, and from the Binational (US-Israel) Science Foundation through Grant No. 2010239. R.C.G. acknowledges support from DMS-1309035. B.P.A. is supported by the National Science Foundation under Grant No. PHY-1205713. P.G.K.'s work at Los Alamos is supported in part by the US Department of Energy. The computations were performed on the HPC cluster HERO, located at the University of Oldenburg and funded by the DFG through its Major Research Instrumentation Programme (INST 184/108-1 FUGG), and by the Ministry of Science and Culture (MWK) of the Lower Saxony State.

- 
- [1] F. Dalfovo, S. Giorgini, L. P. Pitaevskii and S. Stringari, Theory of Bose-Einstein condensation in trapped gases, *Rev. Mod. Phys.* **71**, 463 (1999).
- [2] C. J. Pethick and H. Smith, *Bose-Einstein Condensation in Dilute Gases* (Cambridge University Press, Cambridge, 2002).
- [3] L. P. Pitaevskii and S. Stringari, *Bose-Einstein Condensation* (Oxford University Press, Oxford, 2003).
- [4] B. P. Anderson, P. C. Haljan, C. E. Wieman, and E. A. Cornell, Vortex Precession in Bose-Einstein Condensates: Observations with Filled and Empty Cores, *Phys. Rev. Lett.* **85**, 2857 (2000).
- [5] P. C. Haljan, B. P. Anderson, I. Coddington, and E. A. Cornell, Use of Surface-Wave Spectroscopy to Characterize Tilt Modes of a Vortex in a Bose-Einstein Condensate, *Phys. Rev. Lett.* **86**, 2922 (2001).
- [6] V. Bretin, P. Rosenbusch, F. Chevy, G. V. Shlyapnikov, and J. Dalibard, Quadrupole Oscillation of a Single-Vortex Bose-Einstein Condensate: Evidence for Kelvin Modes, *Phys. Rev. Lett.* **90**, 100403 (2003).
- [7] T. W. Neely, E. C. Samson, A. S. Bradley, M. J. Davis, and B. P. Anderson, Observation of Vortex Dipoles in an Oblate Bose-Einstein Condensate, *Phys. Rev. Lett.* **104**, 160401 (2010).
- [8] D. V. Freilich, D. M. Bianchi, A. M. Kaufman, T. K. Langin, and D. S. Hall, Real-time dynamics of single vortex lines and vortex dipoles in a Bose-Einstein condensate, *Science* **329**, 1182 (2010).
- [9] S. Middelkamp, P. J. Torres, P. G. Kevrekidis, D. J. Frantzeskakis, R. Carretero-González, P. Schmelcher, D. V. Freilich, and D. S. Hall, Guiding-center dynamics of vortex dipoles in Bose-Einstein condensates, *Phys. Rev. A* **84**, 011605(R) (2011).
- [10] R. Navarro, R. Carretero-González, P. J. Torres, P. G. Kevrekidis, D. J. Frantzeskakis, M. W. Ray, E. Altuntaş, and D. S. Hall, Dynamics of a Few Corotating Vortices in Bose-Einstein Condensates, *Phys. Rev. Lett.* **110**, 225301 (2013).
- [11] P. Engels, I. Coddington, P. C. Haljan, and E. A. Cornell, Nonequilibrium Effects of Anisotropic Compression Applied to Vortex Lattices in Bose-Einstein Condensates, *Phys. Rev. Lett.* **89**, 100403 (2002).
- [12] I. Coddington, P. Engels, V. Schweikhard, and E. A. Cornell, Observation of Tkachenko Oscillations in Rapidly Rotating Bose-Einstein Condensates, *Phys. Rev. Lett.* **91**, 100402 (2003).
- [13] N. L. Smith, W. H. Heathcote, J. M. Krueger, and C. J. Foot, Experimental Observation of the Tilting Mode of an Array of Vortices in a Dilute Bose-Einstein Condensate, *Phys. Rev. Lett.* **93**, 080406 (2004).
- [14] V. Schweikhard, I. Coddington, P. Engels, S. Tung, and E. A. Cornell, Vortex-Lattice Dynamics in Rotating Spinor Bose-Einstein Condensates, *Phys. Rev. Lett.* **93**, 210403 (2004).
- [15] S. Tung, V. Schweikhard, and E. A. Cornell, Observation of Vortex Pinning in Bose-Einstein Condensates, *Phys. Rev. Lett.* **97**, 240402 (2006).
- [16] Y. Shin, M. Saba, M. Vengalattore, T. A. Pasquini, C. Sanner, A. E. Leanhardt, M. Prentiss, D. E. Pritchard, and W. Ketterle, Dynamical Instability of a Doubly Quantized Vortex in a Bose-Einstein Condensate, *Phys. Rev. Lett.* **93**, 160406 (2004).
- [17] T. Isoshima, M. Okano, H. Yasuda, K. Kasa, J. A. M. Huhtamäki, M. Kumakura, and Y. Takahashi, Spontaneous Splitting of a Quadruply Charged Vortex, *Phys. Rev. Lett.* **99**, 200403 (2007).
- [18] B. P. Anderson, P. C. Haljan, C. A. Regal, D. L. Feder, L. A. Collins, C. W. Clark, and E. A. Cornell, Watching Dark Solitons Decay into Vortex Rings in a Bose-Einstein Condensate, *Phys. Rev. Lett.* **86**, 2926 (2001).
- [19] Z. Dutton, M. Budde, C. Slowe, and L. V. Hau, Observation of quantum shock waves created with ultra-compressed slow light pulses in a Bose-Einstein condensate, *Science* **293**, 663 (2001).
- [20] M. J. H. Ku, B. Mukherjee, T. Yefsah and M. W. Zwierlein, From planar solitons to vortex rings and lines: Cascade of solitonic excitations in a superfluid Fermi gas, *arXiv:1507.01047*.
- [21] E. A. L. Henn, J. A. Seman, G. Roatı, K. M. F. Magalhães, and V. S. Bagnato, Emergence of Turbulence in an Oscillating Bose-Einstein Condensate, *Phys. Rev. Lett.* **103**, 045301 (2009).
- [22] T. W. Neely, A. S. Bradley, E. C. Samson, S. J. Rooney, E. M. Wright, K. J. H. Law, R. Carretero-González, P. G. Kevrekidis, M. J. Davis, and B. P. Anderson, Characteristics of Two-Dimensional Quantum Turbulence in a Compressible Superfluid, *Phys. Rev. Lett.* **111**, 235301 (2013).
- [23] K. E. Wilson, Z. L. Newman, J. D. Lowney, and B. P. Anderson, *In situ* imaging of vortices in Bose-Einstein condensates, *Phys. Rev. A* **91**, 023621 (2015).
- [24] B. P. Anderson, Resource article: Experiments with vortices in superfluid atomic gases, *J. Low Temp. Phys.* **161**, 574 (2010).
- [25] V. Koukoulouyannis, G. Voyatzis, and P. G. Kevrekidis, Dynamics of three noncorotating vortices in Bose-Einstein condensates, *Phys. Rev. E* **89**, 042905 (2014).

- [26] N. Kyriakopoulos, V. Koukouloyannis, C. Skokos, and P. G. Kevrekidis, Chaotic behavior of three interacting vortices in a confined Bose-Einstein condensate, *Chaos* **24**, 024410 (2014).
- [27] R. H. Goodman, P. G. Kevrekidis, and R. Carretero-González, Dynamics of vortex dipoles in anisotropic Bose-Einstein condensates, *SIAM J. Appl. Dyn. Syst.* **14**, 699 (2015).
- [28] E. C. Samson, K. E. Wilson, Z. L. Newman, and B. P. Anderson, Deterministic creation, pinning, and manipulation of quantized vortices in a Bose-Einstein condensate, *Phys. Rev. A* **93**, 023603 (2016).
- [29] I. Hans, J. Stockhofe, and P. Schmelcher, Generating, dragging, and releasing dark solitons in elongated Bose-Einstein condensates, *Phys. Rev. A* **92**, 013627 (2015).
- [30] *Quantum Gases: Finite Temperature and Non-Equilibrium Dynamics*, edited by N. Proukakis, S. Gardiner, M. Davis, and M. Szymańska (Imperial College Press, London, 2013).
- [31] R. A. Duine, B. W. A. Leurs, and H. T. C. Stoof, Noisy dynamics of a vortex in a partially Bose-Einstein condensed gas, *Phys. Rev. A* **69**, 053623 (2004).
- [32] S. J. Rooney, T. W. Neely, B. P. Anderson, and A. S. Bradley, Persistent-current formation in a high-temperature Bose-Einstein condensate: An experimental test for classical-field theory, *Phys. Rev. A* **88**, 063620 (2013).
- [33] D. Yan, R. Carretero-González, D. J. Frantzeskakis, P. G. Kevrekidis, N. P. Proukakis, and D. Spirn, Exploring vortex dynamics in the presence of dissipation: Analytical and numerical results, *Phys. Rev. A* **89**, 043613 (2014).
- [34] P. G. Kevrekidis, D. J. Frantzeskakis, and R. Carretero-González, *The Defocusing Nonlinear Schrödinger Equation: From Dark Solitons to Vortices and Vortex Rings* (SIAM, Philadelphia, 2015).
- [35] G. Moon, W. J. Kwon, H. Lee, and Y.-I. Shin, Thermal friction on quantum vortices in a Bose-Einstein condensate, *Phys. Rev. A* **92**, 051601(R) (2015).
- [36] L. F. Shampine and M. K. Gordon, *Computer Solution of Ordinary Differential Equations* (Freeman and Company, San Francisco, 1975).
- [37] K. J. H. Law, T. W. Neely, P. G. Kevrekidis, B. P. Anderson, A. S. Bradley, and R. Carretero-González, Dynamic and energetic stabilization of persistent currents in Bose-Einstein condensates, *Phys. Rev. A* **89**, 053606 (2014); see also M. C. Davis, R. Carretero-González, Z. Shi, K. J. H. Law, P. G. Kevrekidis, and B. P. Anderson, Manipulation of vortices by localized impurities in Bose-Einstein condensates, *ibid.* **80**, 023604 (2009).
- [38] P. J. Torres, P. G. Kevrekidis, D. J. Frantzeskakis, R. Carretero-González, P. Schmelcher, and D. S. Hall, Dynamics of Vortex Dipoles in Confined Bose-Einstein Condensates, *Phys. Lett. A* **375**, 3044 (2011).
- [39] S. P. Cockburn, H. E. Nistazakis, T. P. Horikis, P. G. Kevrekidis, N. P. Proukakis, and D. J. Frantzeskakis, Fluctuating and dissipative dynamics of dark solitons in quasicondensates, *Phys. Rev. A* **84**, 043640 (2011).
- [40] C. Becker, S. Stellmer, P. Soltan-Panahi, S. Dörscher, M. Baumert, E.-M. Richter, J. Kronjäger, K. Bongs, and K. Sengstock, Oscillations and interactions of dark and dark-bright solitons in Bose-Einstein condensates, *Nat. Phys.* **4**, 496 (2008); S. Stellmer, C. Becker, P. Soltan-Panahi, E.-M. Richter, S. Dörscher, M. Baumert, J. Kronjäger, K. Bongs, and K. Sengstock, Collisions of Dark Solitons in Elongated Bose-Einstein Condensates, *Phys. Rev. Lett.* **101**, 120406 (2008); C. Becker, K. Sengstock, P. Schmelcher, P. G. Kevrekidis and R. Carretero-González, Inelastic collisions of solitary waves in anisotropic Bose-Einstein condensates: Sling-shot events and expanding collision bubbles, *New J. Phys.* **15**, 113028 (2013).
- [41] C. Ryu, M. F. Andersen, P. Cladé, V. Natarajan, K. Helmerson, and W. D. Phillips, Observation of Persistent Flow of a Bose-Einstein Condensate in a Toroidal Trap, *Phys. Rev. Lett.* **99**, 260401 (2007).
- [42] T. P. Billam, M. T. Reeves, B. P. Anderson, and A. S. Bradley, Onsager-Kraichnan Condensation in Decaying Two-Dimensional Quantum Turbulence, *Phys. Rev. Lett.* **112**, 145301 (2014).
- [43] S. Middelkamp, P. G. Kevrekidis, D. J. Frantzeskakis, R. Carretero-González, and P. Schmelcher, Stability and dynamics of matter-wave vortices in the presence of collisional inhomogeneities and dissipative perturbations, *J. Phys. B: At. Mol. Opt. Phys.* **43**, 155303 (2010).
- [44] M. T. Reeves, T. P. Billam, B. P. Anderson, and A. S. Bradley, Signatures of coherent vortex structures in a disordered two-dimensional quantum fluid, *Phys. Rev. A* **89**, 053631 (2014).
- [45] J. Stockhofe, S. Middelkamp, P. G. Kevrekidis and P. Schmelcher, Impact of anisotropy on vortex clusters and their dynamics, *Europhys. Lett.* **93**, 20008 (2011).
- [46] A. M. Barry, F. Hajir, P. G. Kevrekidis, Generating functions, polynomials, and vortices with alternating signs in Bose-Einstein condensates, *J. Phys. A* **48**, 155205 (2015).
- [47] N. Proukakis, S. Gardiner, M. Davis, and M. Szymanska, *Quantum Gases: Finite Temperature and Non-Equilibrium Dynamics* (Imperial College Press, London, 2013).
- [48] Note that the actual experiments use  $\omega_r = 2\pi \times 8$  Hz [28].